

# An Adaptive GDSW Coarse Space for Two-Level Overlapping Schwarz Methods in Two Dimensions

Alexander Heinlein<sup>1</sup>, Axel Klawonn<sup>1</sup>, Jascha Knepper<sup>1</sup>, and Oliver Rheinbach<sup>2</sup>

## 1 Introduction

We consider the second order elliptic problem in two dimensions

$$\begin{aligned} -\nabla \cdot (A(x)\nabla u(x)) &= f(x) && \text{in } \Omega \subset \mathbb{R}^2, \\ u &= 0 && \text{on } \partial\Omega, \end{aligned} \tag{1}$$

where the scalar coefficient function  $A(x) > 0$  is highly heterogeneous, possibly with high jumps. While convergence of standard two-level Schwarz preconditioners depends on the contrast of the coefficient function, we propose a coarse space for two-level overlapping Schwarz methods which yields a condition number that is independent of the coefficient function. Our approach can be viewed as an extension to the GDSW (Generalized Dryja, Smith, Widlund) method [1, 2] since it always contains the standard GDSW coarse space. Originally, the method was inspired by the ACMS (Approximate Component Mode Synthesis) special finite element method [9, 6], which uses enrichment of the discretization space by local eigenfunctions. The ACMS space was first considered as a coarse space for overlapping Schwarz methods in [7].

Our new coarse space consists of simple nodal finite element functions and of energy minimizing extensions of solutions of generalized eigenvalue problems on the edges. Here, we restrict ourselves to the two-dimensional case. For the description of the three-dimensional case and the proof of the condition number bound, we refer to [8]. A related method is the SHEM (Spectral Harmonically Enriched Multiscale) coarse space, introduced in [5], however, our eigenvalue problems do not use mass matrices; see (5). Other related coarse spaces for overlapping Schwarz methods are,

---

<sup>1</sup>Mathematisches Institut, Universität zu Köln, Weyertal 86-90, 50931 Köln, Germany. e-mail: {alexander.heinlein,axel.klawonn,jascha.knepper}@uni-koeln.de

<sup>2</sup>Institut für Numerische Mathematik und Optimierung, Fakultät für Mathematik und Informatik, Technische Universität Bergakademie Freiberg, Akademiestr. 6, 09596 Freiberg, Germany. e-mail: oliver.rheinbach@math.tu-freiberg.de

e.g., [3, 4]. In our new coarse space and in the one based on the ACMS discretization method, the construction of the generalized eigenvalue problems is computationally slightly more expensive than in the SHEM coarse space [5]. However, the dimension of the coarse space can be reduced significantly in certain cases.

The variational problem corresponding to (1) reads: find  $u \in H_0^1(\Omega)$ , such that

$$a_\Omega(u, v) = L(v) \quad \forall v \in H_0^1(\Omega) \quad (2)$$

with the bilinear form and the linear functional

$$a_\Omega(u, v) := \int_\Omega (\nabla u(x))^T A(x) \nabla v(x) dx \quad \text{and} \quad L(v) := \int_\Omega f(x) v(x) dx,$$

respectively, where  $f \in L^2(\Omega)$ . We define the semi-norm corresponding to the bilinear form  $a_\Omega(\cdot, \cdot)$  as  $|u|_{a, \Omega}^2 := a_\Omega(u, u)$ . Let  $Ku = f$  be the discretization of problem (2) by piecewise linear or bilinear finite elements on a family of triangulations  $(\tau_h)_h$ . We solve the discretized system using the conjugate gradient method preconditioned by a suitable two-level overlapping Schwarz preconditioner.

## 2 The GDSW Preconditioner

The GDSW preconditioner [1, 2] is a two-level additive overlapping Schwarz preconditioner with exact solvers; cf. [10]. It can therefore be written in the form

$$M_{\text{GDSW}}^{-1} = \Phi K_0^{-1} \Phi^T + \sum_{i=1}^N R_i^T \tilde{K}_i^{-1} R_i, \quad (3)$$

where  $K_0 = \Phi^T K \Phi$  and  $\tilde{K}_i = R_i^T K R_i$ . The matrices  $R_i$  are the restriction operators to the overlapping subdomains  $\tilde{\Omega}_i$ ,  $i = 1, \dots, N$ , and the columns of  $\Phi$  are the coarse basis functions. The coarse basis functions are discrete harmonic extensions of interface functions into the interior degrees of freedom of the corresponding nonoverlapping subdomains. On the interface, the values are defined as the restrictions of the nullspace of the operator to the edges and vertices of the nonoverlapping domain decomposition.

The condition number estimate for the GDSW Schwarz operator in case of a constant coefficient function  $A$  is

$$\kappa(M_{\text{GDSW}}^{-1} K) \leq C \left(1 + \frac{H}{\delta}\right) \left(1 + \log\left(\frac{H}{h}\right)\right)^2; \quad (4)$$

cf. [1, 2]. If  $A$  is not constant, the constant  $C$  also depends the contrast of  $A$ .

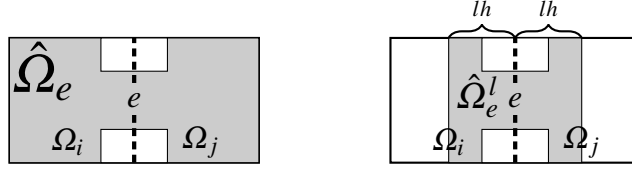


**Fig. 1** (left) Graphical representation of  $\Omega_e = \Omega_i \cup \Omega_j$  and  $\hat{\Omega}_e$ . The set  $\hat{\Omega}_e$  is obtained by removing from  $\Omega_e$  all elements which are adjacent to the coarse nodes. From this, we also obtain the interior edge  $\hat{e} := e \cap \hat{\Omega}_e$ . (right) Graphical representation of the slab  $\hat{\Omega}_e^l$  corresponding to the edge  $e$ .

### 3 Adaptive GDSW in 2D

The adaptive GDSW coarse space is an extension to the standard GDSW coarse space since it automatically includes the standard GDSW coarse space. However, if necessary due to coefficient jumps, additional coarse constraints are selected. These additional coarse constraints are constructed from solving local generalized eigenvalue problems. Let the interface  $\Gamma$  be partitioned into edges  $\mathcal{E}$  and vertices  $\mathcal{V}$ , i.e.,  $\Gamma = (\bigcup_{e \in \mathcal{E}} e) \cup (\bigcup_{v \in \mathcal{V}} v)$ . For each edge  $e$ , we define the sets  $\Omega_e$  and  $\hat{\Omega}_e$  as depicted in Fig. 1 (left) and the following extension operator:

$$w_e : V_0^h(e) \rightarrow V_0^h(\Omega_e), \quad v \mapsto w_e(v) := \begin{cases} v & \text{in all interior nodes of } e, \\ 0 & \text{on all other nodes in } \Omega_e, \end{cases}$$

where  $V_0^h(e) := \{v|_e : v \in V, v = 0 \text{ on } \partial e\}$ . Then, we consider on each edge  $e \in \mathcal{E}$  the generalized eigenvalue problem: find  $\tau_{*,e} \in V_0^h(e)$  such that

$$a_{\hat{\Omega}_e} \left( \mathcal{H}_{\hat{e} \rightarrow \hat{\Omega}_e}(\tau_{*,e}), \mathcal{H}_{\hat{e} \rightarrow \hat{\Omega}_e}(\theta) \right) = \lambda_{*,e} a_{\Omega_e}(w_e(\tau_{*,e}), w_e(\theta)) \quad \forall \theta \in V_0^h(e). \quad (5)$$

Here,  $\mathcal{H}_{\hat{e} \rightarrow \hat{\Omega}_e}$  denotes the discrete harmonic extension from the interior edge  $\hat{e}$  into  $\hat{\Omega}_e$  with respect to the bilinear form  $a_{\hat{\Omega}_e}(\cdot, \cdot)$ . Let the corresponding eigenvalues be sorted in non-descending order, i.e.,  $\lambda_{1,e} \leq \lambda_{2,e} \leq \dots \leq \lambda_{m,e}$ , and the eigenmodes accordingly, where  $m = \dim(V_0^h(e))$ . We select all eigenmodes  $\tau_{*,e}$  where the eigenvalues are below a certain tolerance, i.e.,  $\lambda_{*,e} \leq \text{tol}_{\mathcal{E}}$ . Then we extend the selected eigenfunctions by zero to  $\Gamma \setminus e$ , denoted by  $\tilde{\tau}_{*,e}$ , and subsequently compute the discrete harmonic extension into the interior of the subdomains, i.e.,  $v_{*,e} := \mathcal{H}_{\Gamma \rightarrow \Omega}(\tilde{\tau}_{*,e})$ .

Note that for every edge  $e$ , the left hand side of the eigenvalue problem (5) is singular. Therefore, since  $\text{tol}_{\mathcal{E}} \geq 0$ , eigenmodes which span the nullspace are always selected and added to the coarse space. Therefore, the standard GDSW coarse space is always a subspace of our automatic coarse space.

In addition to the edge basis functions, we use the nodal coarse basis functions from the GDSW coarse space, which span the space  $V_{\mathcal{V}}$ . We denote the resulting coarse space as the AGDSW (Adaptive GDSW) coarse space:

$$V_{\text{AGDSW}}^{\text{tol}_\mathcal{E}} = V_\gamma \oplus \left( \bigoplus_{e \in \mathcal{E}} \text{span} \{v_{k,e} : \lambda_{k,e} \leq \text{tol}_\mathcal{E}\} \right)$$

*Remark 1:* For  $\text{tol}_\mathcal{E} \geq 0$ , we obtain  $V_{\text{GDSW}} = V_{\text{AGDSW}}^0 \subseteq V_{\text{AGDSW}}^{\text{tol}_\mathcal{E}}$ .

*Remark 2:* The right hand side of the eigenvalue problem (5) can be extracted from the fully assembled global stiffness matrix  $K$ .

*Remark 3:* The condition number of the AGDSW Schwarz operator is bounded by

$$\kappa(M_{\text{AGDSW}}^{-1}K) \leq C \left( 1 + \frac{1}{\text{tol}_\mathcal{E}} \right); \quad (6)$$

see [8]. The constant  $C$  is independent of  $H$ ,  $h$ , and the contrast of the coefficient function  $A$ . In [8], the three-dimensional case is also covered including the theory.

## 4 Variants of Adaptive GDSW

Here, we will briefly discuss some possible variants of the AGDSW method.

**Mass matrix** As in other adaptive coarse spaces where a spectral estimate is used to replace a Poincaré type inequality, cf., e.g., [3, 4, 5, 7], we can use a (scaled) mass matrix on the right hand side of the eigenvalue problems. The scaled mass matrix corresponding to an edge  $e \subset (\hat{\Omega}_i \cap \hat{\Omega}_j)$  arises from the discretization of the scaled  $L^2$ -inner product

$$b_e(u, v) := \frac{1}{h^2} (A \cdot w_e(u), w_e(v))_{L^2(\Omega_e)}. \quad (7)$$

Therefore, we obtain for each edge the modified generalized eigenvalue problem: find  $\tau_{*,e} \in V_0^h(e)$  such that

$$a_{\hat{\Omega}_e} \left( \mathcal{H}_{\hat{e} \rightarrow \hat{\Omega}_e}(\tau_{*,e}), \mathcal{H}_{\hat{e} \rightarrow \hat{\Omega}_e}(\theta) \right) = \lambda_{*,e} b_e(\tau_{*,e}, \theta) \quad \forall \theta \in V_0^h(e). \quad (8)$$

The condition number bound (6) can also be proven for this variant; see [8].

**Slabs** In order to reduce the computational cost of constructing the generalized eigenvalue problems, the set  $\hat{\Omega}_e$  can be replaced by a slab of width  $l$  elements around the edge  $e$  in (5); cf. Fig. 1 (right) for the graphical representation of a slab corresponding to the edge  $e$ . We denote the slab by  $\hat{\Omega}_e^l$ . This idea, to use slabs in the eigenvalue problems, has already been introduced in [7] for related multi-scale coarse spaces based on the ACMS space and is also common in FETI-DP and BDDC domain decomposition methods with adaptive coarse spaces.

The modified generalized eigenvalue problem reads: find  $\tau_{*,e} \in V_0^h(e)$  such that

$$a_{\hat{\Omega}_e^l} \left( \mathcal{H}_{\hat{e} \rightarrow \hat{\Omega}_e^l}(\tau_{*,e}), \mathcal{H}_{\hat{e} \rightarrow \hat{\Omega}_e^l}(\theta) \right) = \lambda_{*,e} a_{\Omega_e} (w_e(\tau_{*,e}), w_e(\theta)) \quad \forall \theta \in V_0^h(e). \quad (9)$$

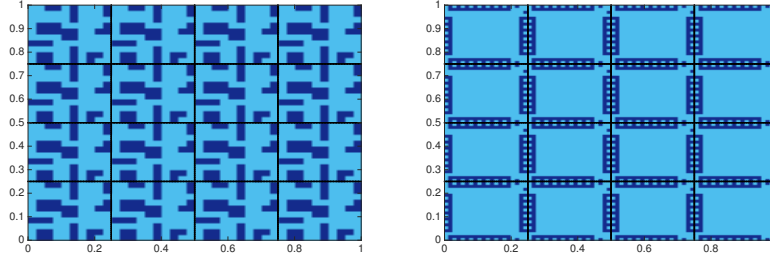


**Fig. 2** Discontinuous coefficient functions  $A$  with different types of channels and inclusions intersecting the interface. Maximum coefficient (dark blue color):  $A_{\max} = 10^6$  (left),  $A_{\max} = 10^8$  (right);  $1/H = 4$ ;  $H/h = 30$  (left);  $H/h = 40$  (right);  $\delta = 2h$ .

$V_0$	Coeff. function $A$ from Fig. 2 (left)				Coeff. function $A$ from Fig. 2 (right)			
	$tol_{\mathcal{E}}$	it.	$\kappa$	$\dim V_0$	$tol_{\mathcal{E}}$	it.	$\kappa$	$\dim V_0$
$V_{\text{GDSW}}$		264	$1.04 \cdot 10^6$	33		45	26.18	33
$V_{\text{AGDSW}}$	$10^{-1}$	29	7.15	93	$10^{-1}$	34	10.06	81
	$10^{-2}$	29	7.15	93	$10^{-2}$	44	26.20	57
$V_{\text{AGDSW-M}}$	$10^{-1}$	29	7.15	93	$10^{-1}$	44	26.20	57
	$10^{-2}$	29	7.15	93	$10^{-2}$	44	26.20	57
$V_{\text{SHEM}}$	$10^{-3}$	20	4.33	69	$10^{-3}$	23	5.03	213
	$10^{-6}$	20	4.33	69	$10^{-6}$	23	5.03	213

**Table 1** Results for the coefficient functions in Fig. 2: tolerance for the selection of the eigenfunctions, iterations counts, condition numbers, and resulting coarse space dimension for different coarse space variants;  $1/H = 4$ ,  $H/h = 30$  (left),  $H/h = 40$  (right), and  $\delta = 2h$ ; maximum coefficient  $A_{\max} = 10^6$  (left) and  $A_{\max} = 10^8$  (right).

The slab variant is computationally cheaper and the bound can be proven analogously to the standard version with no modifications. However, the coarse space dimension can increase due to the use of this variant (if  $\hat{\Omega}_e^l \subset \hat{\Omega}_e$ ).

## 5 Numerical Results

We present numerical results for model problem (1) for  $f \equiv 1$  and various coefficient functions, comparing the different AGDSW approaches with the standard GDSW as well as the SHEM coarse space, recently introduced by Gander, Loneland, and Rahman in [5]. Finally, we show results using slabs of varying widths.

In all figures, the light and dark blue colors correspond to the minimum coefficient ( $A_{\min} = 1.0$ ) and maximum coefficient ( $A_{\max} = 10^6$  or  $A_{\max} = 10^8$ ), respectively. We use piecewise bilinear finite elements, and solve the discrete linear system using the conjugate gradient method with a relative stopping criterion,  $\|r^{(k)}\|_2 / \|r^{(0)}\|_2 \leq 10^{-8}$ , where  $r^{(0)}$  and  $r^{(k)}$  are the initial and the  $k$ -th unpreconditioned residual, respectively. By  $V_{\text{GDSW}}$ , we denote the standard GDSW space and by  $V_{\text{AGDSW}}^{tol}$  the new adaptive GDSW coarse space. The variant which uses a scaled

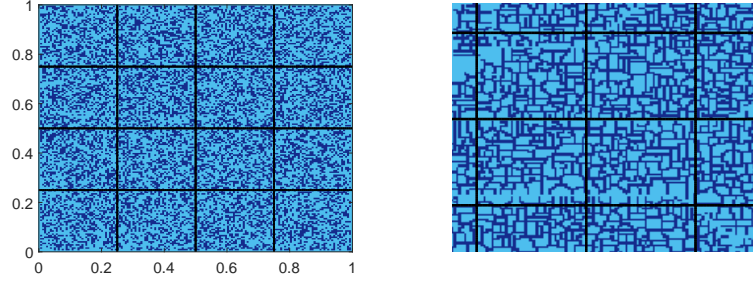


**Fig. 3 (Left:)** Sample random coefficient function with a density of approximately 40% high coefficients  $A_{\max} = 10^6$  (dark blue color).  $1/H = 4$ ;  $H/h = 40$ ;  $\delta = 1h$ . **(Right:)** Detailed view of a coefficient function with  $A_{\max} = 10^8$  (dark blue color) and  $1/H = 20$ ,  $H/h = 40$ ,  $\delta = 1h$ .

$V_0$	Random coeff. function $A$ from Fig. 3 (left)				Coeff. fn. $A$ from Fig. 3 (right)			
	$tol_{\mathcal{E}}$	it.	$\kappa$	$\dim V_0$	$tol_{\mathcal{E}}$	it.	$\kappa$	$\dim V_0$
$V_{\text{GDSW}}$	$> 500$ ( - )	$2.8 \cdot 10^5$ ( $6.9 \cdot 10^4$ )		33 ( 0.0)	3 042	$4.9 \cdot 10^7$	1 121	
$V_{\text{AGDSW}}$	$10^{-1}$	34.3 ( 1.7)	11.8 ( 2.0)	185.1 ( 7.0)	$10^{-1}$	47	16.2	3 087
$V_{\text{AGDSW-M}}$	$10^{-1}$	51.6 ( 3.7)	22.6 ( 7.6)	148.4 ( 8.5)	$10^{-1}$	75	40.1	1 862
$V_{\text{AGDSW}}$					$5 \cdot 10^{-2}$	62	28.5	2 257
$V_{\text{AGDSW-M}}$					$5 \cdot 10^{-2}$	85	59.4	1 706
$V_{\text{AGDSW}}$	$10^{-2}$	78.9 ( 6.4)	81.7 ( 25.1)	127.7 ( 9.5)	$10^{-2}$	92	97.2	1 702
$V_{\text{AGDSW-M}}$	$10^{-2}$	112.2 (11.6)	119.5 ( 44.8)	181.1 (10.7)	$10^{-2}$	92	97.2	1 702
$V_{\text{SHEM}}$	$10^{-3}$	36.6 ( 3.3)	18.2 ( 6.8)	215.0 ( 8.4)	$10^{-2}$	48	19.9	4 450
$V_{\text{SHEM}}$	$10^{-6}$	80.1 (28.2)	14 283.8 (15 740.5)	189.2 ( 8.1)	$10^{-4}$	60	32.3	4 324

**Table 2** Results for the coefficient functions in Fig. 3: tolerance for the selection of the eigenfunctions, iteration counts, condition numbers, and resulting coarse space dimension for different coarse space variants. **(Left:)** Averaged results for 100 random coefficient functions ( $\approx 40\%$  density); standard deviation in brackets. GDSW never converged within the maximum iteration number of 500.  $1/H = 4$ ,  $H/h = 40$ , and  $\delta = 1h$ ; maximum coefficient  $A_{\max} = 10^6$ . **(Right:)**  $1/H = 20$ ;  $H/h = 40$ ;  $\delta = 1h$ ; maximum coefficient  $A_{\max} = 10^8$ .

mass matrix in the right hand side of the eigenvalue problem, cf. section 4, is denoted by  $V_{\text{AGDSW-M}}^{\text{tol}}$ , the variant using a slab of width  $w = lh$  is denoted by  $V_{\text{AGDSW-E}(l)}^{\text{tol}}$ , and the SHEM coarse space by  $V_{\text{SHEM}}^{\text{tol}}$ ; cf. [5].

In Table 1, we compare the different coarse spaces for the two coefficient functions illustrated in Fig. 2. It is evident that, for the coefficient function from Fig. 2 (left), the GDSW coarse space is not sufficient to yield a low condition number and a small number of iterations; see Table 1 (left). This is due to multiple disconnected, high coefficient channels and inclusions intersecting the interface. However, the GDSW coarse space is sufficient for the coefficient function from Fig. 2 (right); see Table 1 (right). Here, only one connected high coefficient component exists per edge, all other high coefficient components are entirely contained in the overlap. Let us remark that a reduction of the overlap to one element, i.e.,  $\delta = 1h$ , and only using the standard GDSW coarse space leads to 207 iterations and a condition number of  $8.97 \cdot 10^7$ . In Table 1, all adaptive methods achieve low condition numbers and

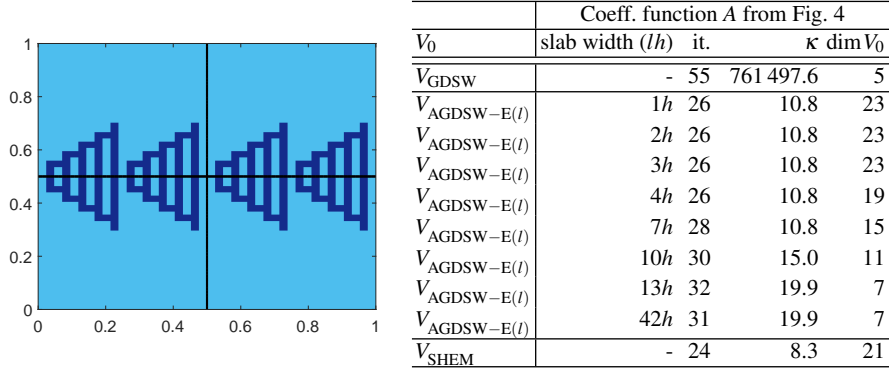


**Fig. 4** Coefficient function with many connected channels intersecting the interface. Maximum coefficient  $A_{\max} = 10^6$  (dark blue);  $1/H = 2$ ;  $H/h = 42$ ;  $\delta = 2h$ .

**Table 3** Results for the coefficient function in Fig. 4: slab width, iterations counts, condition numbers, and resulting coarse space dimension for different coarse space variants. A tolerance for the selection of the eigenfunctions of  $10^{-3}$  was used for  $V_{\text{AGDSW-E}(l)}$  and  $V_{\text{SHEM}}$ ;  $1/H = 2$ ,  $H/h = 42$ , and  $\delta = 2h$ ; maximum coefficient  $A_{\max} = 10^6$ .

converge in few iterations for both coefficient functions. For the coefficient function from Fig. 2 (left), both adaptive GDSW coarse spaces have higher coarse space dimensions compared to the SHEM coarse spaces. This can be explained as follows: first, the entire GDSW coarse space is always included in the AGDSW coarse space and second, all high coefficient components intersecting the interface are disconnected. For the coefficient function from Fig. 2 (right), many channels of high coefficients intersecting the interface are connected. Here, the coarse space  $V_{\text{SHEM}}^{10^{-6}}$  has a dimension of 213, where both AGDSW approaches lead to a significantly lower coarse space dimension of 57 using a tolerance of  $10^{-2}$ .

In Fig. 3 (left), a randomly generated coefficient function is displayed. Averaged results for 100 random coefficient functions are listed in Table 2 (left). The coefficient functions are constructed as follows: uniformly distributed numbers are randomly generated in the interval  $[0, 1]$ . A value above 0.6 corresponds to a high coefficient  $A_{\max} = 10^6$  in a finite element. Otherwise the coefficient is set to  $A_{\min} = 1.0$ . The coefficient of an element that touches the global domain boundary is always set to  $A_{\min}$ .

The results in Table 2 (left) show that all adaptive coarse spaces (AGDSW and SHEM) yield low condition numbers and numbers of iterations. On average, compared to the SHEM coarse space, for these problems, the adaptive GDSW approaches have lower coarse space dimensions. For example,  $V_{\text{SHEM}}^{10^{-6}}$  and  $V_{\text{AGDSW}}^{10^{-2}}$  converge in approximately the same number of iterations, i.e., 80.1 and 78.9, respectively. However,  $V_{\text{SHEM}}^{10^{-6}}$  has a coarse space dimension of 189.2, whereas the dimension of  $V_{\text{AGDSW}}^{10^{-2}}$  is 127.7. This corresponds to a reduction by 33 percent.

We also consider a foam-like coefficient function, as depicted in Fig. 3 (right). The results in Table 2 (right) show that a robust preconditioner, with additional coarse constraints, is needed as  $V_{\text{GDSW}}$  requires over 3 000 iterations to converge. The adaptive GDSW variants and  $V_{\text{SHEM}}$  need few iterations to converge. However,  $V_{\text{SHEM}}^{10^{-4}}$  requires a much larger coarse space, of dimension 4 324, compared to  $V_{\text{AGDSW}}^{5 \cdot 10^{-2}}$ , dimension 2 257, while requiring approximately the same number of iterations to converge. This corresponds to a reduction by 48 percent.

We now investigate the use of different slab widths in the variant  $V_{\text{AGDSW-E}(l)}$ ; cf. section 4. We are able to reduce the computational cost by using small slabs. However, when the detection of connected high coefficient components is weakened, we may enlarge the coarse space. This can be observed clearly for the coefficient function in Fig. 4. Increasing the slab width decreases the resulting coarse space dimension for  $V_{\text{AGDSW-E}(l)}$ ; also cf. Table 3. In this particular example, a slab width of 13 is sufficient to achieve the same result as with the maximum slab width of 42 since the slab then contains only two high coefficient components per edge.

## References

1. Clark R. Dohrmann, Axel Klawonn, and Olof B. Widlund. Domain decomposition for less regular subdomains: overlapping Schwarz in two dimensions. *SIAM J. Numer. Anal.*, 46(4):2153–2168, 2008.
2. Clark R. Dohrmann, Axel Klawonn, and Olof B. Widlund. A family of energy minimizing coarse spaces for overlapping Schwarz preconditioners. In *Domain decomposition methods in science and engineering XVII*, volume 60 of *Lect. Notes Comput. Sci. Eng.*, pages 247–254. Springer, Berlin, 2008.
3. Victorita Dolean, Frédéric Nataf, Robert Scheichl, and Nicole Spillane. Analysis of a two-level Schwarz method with coarse spaces based on local Dirichlet-to-Neumann maps. *Comput. Methods Appl. Math.*, 12(4):391–414, 2012.
4. Juan Galvis and Yalchin Efendiev. Domain decomposition preconditioners for multiscale flows in high-contrast media. *Multiscale Modeling & Simulation*, 8(4):1461–1483, 2010.
5. Martin J. Gander, Atle Loneland, and Talal Rahman. Analysis of a new harmonically enriched multiscale coarse space for domain decomposition methods. Technical report, arxiv.org. 16 Dec 2015.
6. Alexander Heinlein, Ulrich Hetmaniuk, Axel Klawonn, and Oliver Rheinbach. The approximate component mode synthesis special finite element method in two dimensions: Parallel implementation and numerical results. *J. Computat. Appl. Math.*, Vol. 289:116–133, 2015.
7. Alexander Heinlein, Axel Klawonn, Jascha Knepper, and Oliver Rheinbach. Multiscale coarse spaces for overlapping Schwarz methods based on the ACMS space in 2D. Technical Report Preprint 2016-09 at <http://tu-freiberg.de/fakult1/forschung/preprints>, Technische Universität Bergakademie Freiberg, Fakultät für Mathematik und Informatik, 2016. Submitted 08/2016 to ETNA.
8. Alexander Heinlein, Axel Klawonn, Jascha Knepper, and Oliver Rheinbach. Adaptive GDSW. Technical report, 2017. In Preparation.
9. Ulrich Hetmaniuk and Richard B. Lehoucq. A special finite element method based on component mode synthesis. *ESAIM: Mathematical Modelling and Numerical Analysis*, 44(3):401–420, 4 2010.
10. Andrea Toselli and Olof Widlund. *Domain decomposition methods—algorithms and theory*, volume 34 of *Springer Series in Computational Mathematics*. Springer-Verlag, Berlin, 2005.